RAA 2021 Vol. **21** No. **7**, 157(6pp) doi:10.1088/1674-4527/21/7/157
© 2021 National Astronomical Observatories, CAS and IOP Publishing Ltd.
http://www.raa-journal.org *http://iopscience.iop.org/raa*

***R**esearch in*
***A**stronomy and*
***A**strophysics*

Research on actuator distribution and panels for a radio telescope

Jin-Qing Wang[1,2,3], Zheng-Xiong Sun[1], Li Fu[1,2,3], Jin-Ling Li[1], Lin-Feng Yu[1,2,3], Yong-Chen Jiang[1,2,3],Yong-Bin Jiang[1,2,3], Wei Gou[1], Wei Hu[1,4], Rong-Bin Zhao[1,2,3], Qin-Hui Liu[1,2,3] and Zhi-Qiang Shen[1,2,3]

[1] Shanghai Astronomical Observatory, Chinese Academy of Sciences, Shanghai 200030, China; *jqwang@shao.ac.cn*
[2] Key Laboratory of Radio Astronomy, Chinese Academy of Sciences, Nanjing 210008, China
[3] Shanghai Key Laboratory of Space Navigation and Positioning Techniques, Shanghai 430074, China
[4] University of Shanghai for Science and Technology, Shanghai 200093, China

Received 2021 January 4; accepted 2021 January 25

Abstract Trying to achieve the best surface accuracy control with the fewest actuators, this article mainly studies the distribution of actuators and the method of panel design. The influence of the number of faulty actuators on the accuracy of the surface shape is demonstrated. In addition, the method incorporating a triangular panel, node index and the fitting solution method of a single panel is also given. This method provides a reference for the design and realization of an active surface or a deformable sub-reflector for high performance large aperture radio telescopes.

Key words: radio telescope — triangle panel — method — design

1 INTRODUCTION

An active surface system can effectively eliminate the surface error that is caused by gravitational or thermal deformation (Wang et al. 2019; Dong et al. 2018). Although it should ideally maintain a parabolic shape, the number of actuators is very large. Take the Tianma 65 meter antenna as an example, it is composed of 1104 actuators. The large number of actuators poses a great challenge to the reliability of the system. This paper studies the distribution of actuators, the influence of faulty actuators on the surface shape accuracy, as well as the panel design to reduce actuators. The panel adjustment fitting model is also given. This method is suitable for the top design of a radio telescope which is equipped with an active surface or deformable sub-reflector (Wang et al. 2020).

2 ACTUATOR DISTRIBUTION

Taking the Tianma 65 meter case as a reference, the active surface is designed with 1104 actuator positions. This paper simulates the optimal distribution of the actuators on the entire surface when the number of actuators is limited. It provides a basis for the subsequent development of using a smaller number of actuators to form an active surface or a deformable sub-reflector. The algorithm model for solving the optimal number and distribution of the actuators is diagrammed in Figure 1. Under normal circumstances, an aperture illumination distribution with a tapering of about 10 dB is usually applied for large radio telescopes. This is mainly to suppress sidelobe reception and reduce noise, but this will also cause some loss in gain. For large antennas that receive data from deep space, in order to maximize the gain, a uniform aperture distribution is applied although the noise will increase (Wang et al. 2020).

Figure 2 displays the 10 dB taper aperture illumination function and the Finite Element Method (FEM) simulation adjustment of each actuator over the entire range of elevation. The multiplication of the two data above is used as the weight function to make the decision of actuators' arrangement and all actuators are prioritized. Figure 3 illustrates the optimal placement of 400, 600 and 800 actuators, from left to right respectively. Table 1 shows the reduction in the aperture efficiency at each elevation under the compensation of different numbers of actuators, which was calculated by the Lutz formula (Ruze 1966), as expressed in Equation (1). Here λ is the wavelength and ε (mm) represents surface accuracy of a parabolic antenna. The 57 degree elevation is the best position which is used as the normalized efficiency.

$$\eta = \exp\left[-\left(\frac{4\pi\varepsilon}{\lambda}\right)^2\right] \quad (1)$$

Figure 4 plots the efficiency loss of the aperture surface efficiency at each elevation with compensation

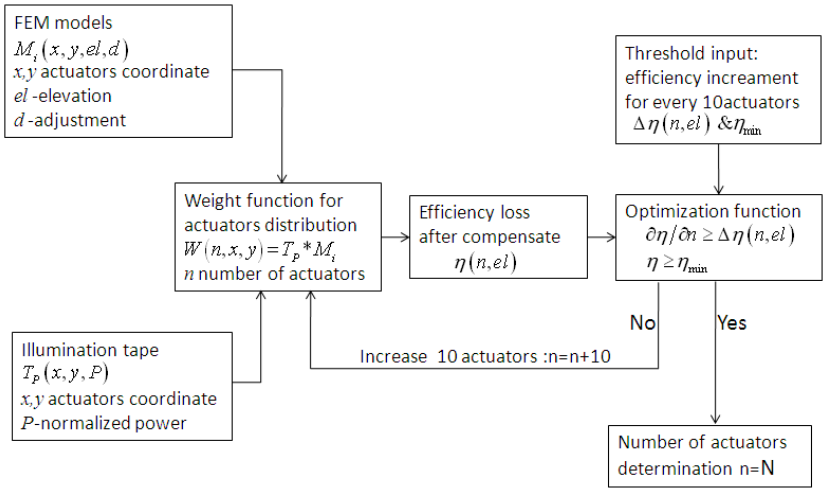

Fig. 1 Optimized number of actuators and distribution model.

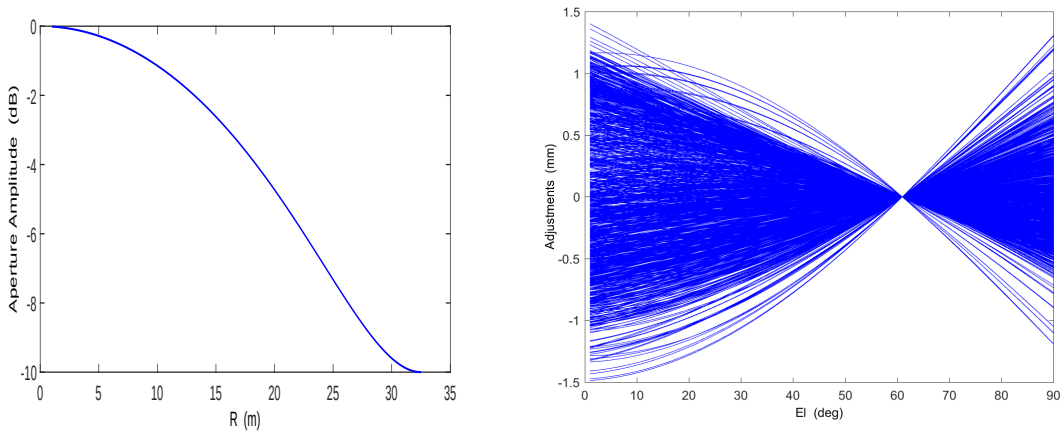

Fig. 2 *Left*: Aperture illumination function; *Right*: Compensation of 1104 actuators over entire elevation.

Table 1 The Decrease of Gain (Efficiency) Before and After Compensation by Different Numbers of Actuators

EL (°)	17	27	37	47	57	67	77	87	Number
Before	0.45	0.6	0.76	0.91	0.99	0.98	0.88	0.70	0
	0.626	0.741	0.853	0.944	0.995	0.989	0.919	0.795	300
	0.681	0.784	0.880	0.955	0.996	0.991	0.934	0.829	400
	0.741	0.830	0.907	0.966	0.997	0.993	0.947	0.860	500
After	0.809	0.877	0.934	0.976	0.998	0.995	0.960	0.890	600
	0.881	0.927	0.961	0.985	0.999	0.996	0.973	0.923	700
	0.937	0.964	0.981	0.993	0.999	1.0	0.982	0.942	800
	0.965	0.983	0.992	0.996	1.0	0.998	0.987	0.956	900
	0.984	0.995	0.997	0.998	1.0	0.999	0.990	0.965	1000

by different numbers of actuators. It can be seen that when the number of actuators reaches more than 600, the gain loss in high and low elevation is already better than 80%. If the best efficiency is 60%, it can reach more than 48% at high and low elevation. It can be seen from Figure 3 that even the smallest distribution of 400 actuators presents a concentrated distribution of six large areas. This is advantageous for relying on the sub-reflector to compensate for gravity deformation of the main surface. The diameter of the sub-reflector of the Tianma facility is 1/10 of the diameter of the main surface. It can be roughly estimated that the number of main surface actuators used is about 1/10 of the main surface. That means 80 actuators for sub-reflector compensation can almost achieve 90% performance of the 800 actuators on the main surface mentioned above.

In order to obtain the exact number of optimized actuators, we propose to optimize the number on the basis

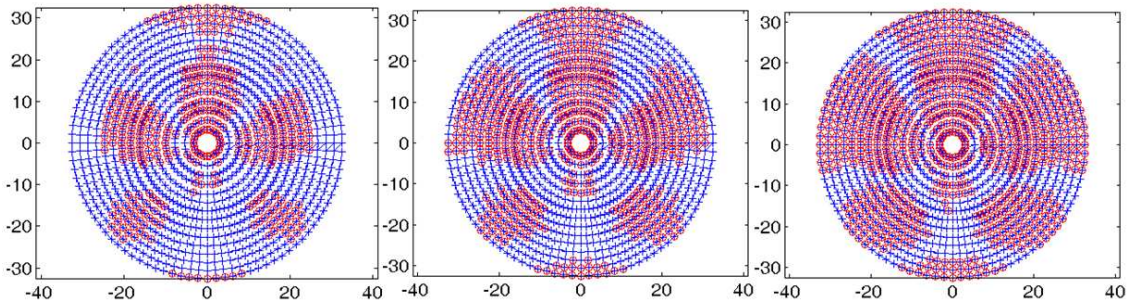

Fig. 3 Red circles mean the location of the actuators. *Left*: the optimal distribution of 400 actuators; *Middle*: the optimal distribution of 600 actuators; *Right*: The final distribution of 800 actuators.

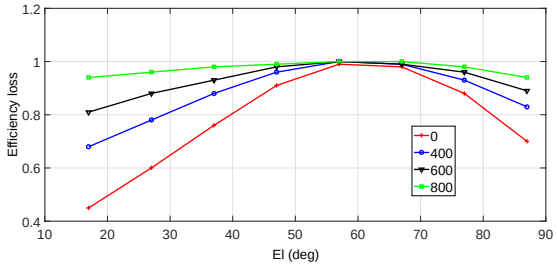

Fig. 4 The efficiency loss of the aperture surface efficiency over the entire elevation with compensation by different numbers of actuators.

of the above-mentioned optimal distribution of actuators. The basic criterion is the increase in efficiency caused by every 10 actuators and the minimum permitted efficiency. The rate of change in efficiency at the lowest or highest elevation is most easily judged, which we used as the basis. From Figure 4, we derive the relationship between the efficiency loss and the number of actuators at elevation of 17 deg, as featured in Figure 5. Then we derive the efficiency improvement caused by every 10 actuators, as depicted in Figure 6. It demonstrates that when the number of actuators is between 300 and 800, every additional 10 actuators can achieve more than 0.45% increment. The most efficient number of actuators is about 550, and every additional 10 actuators can improve the efficiency by about 0.7%. Even at the number 800, there is still an improvement of about 0.45%, but after 900 actuators, the efficiency of each additional 10 actuators is less than 0.25%. It can be seen that if we take the 0.45% efficiency improvement for every 10 actuators as the threshold, we can get the optimal number of actuators to be about 800.

3 THE INFLUENCE OF A FAULTY ACTUATOR ON SURFACE ACCURACY

Take the Shanghai Tianma 65 meter radio telescope as an example. There are 1008 panels and 1104 actuators. Under the condition that the illumination function is evenly distributed and with a tapering of about 10 dB, we analyze the working mode of an actuator connecting the corner of four panels. We also suppose the accuracy of the main surface accuracy is 0.3 mm when there are no broken actuators. At the same time, assuming that the positioning standard deviation of a single faulty actuator is a random distribution of 5 mm, the simulation now randomly generates n ($1 < n < 250$) as the number of random faulty actuators, and the position error of the remaining $1104 - n$ actuators is 0.3 mm. The installation and distribution positions of the actuators on the Tianma 65 m aperture are illustrated in Figure 7, which are also given as random positions. While considering the adjacent effect, in general, a faulty actuator will cause the error in the four panels to deteriorate. However, if two actuators are broken and if the actuators are adjacent to each other, the accuracy of six panels will deteriorate instead of eight panels. Using the illumination function on the aperture and the panel area on each ring as the weighting factor, the adjustment errors of the actuators are multiplied by the weighting factor. And finally, the standard deviation of 1104 data is counted as the n^{th} aperture deviation error. After 250 repeated runnings we can get 250 aperture deviations. The result is as displayed in Figure 8, where black means the aperture surface illumination is uniformly distributed, regardless of the area of each ring panel. Blue points connote that the illumination distribution is a 10 dB tape, not counting the aperture amplitude of each rings' panels. Red points signify that the illumination distribution is a 10 dB taper and the panels' area weights are all considered. It can be seen that in the case of uniform lighting distribution and a few faulty actuators at the beginning, the overall main surface statistical accuracy deteriorates rapidly. When there are ten dead actuators, the surface error has reached 0.5 mm. After the number has risen to fifty, as the probability of adjacent dead actuators increases, the deterioration speed begins to slow down. When considering the aperture illumination and the panels' size in the different rings, this deterioration speed will be significantly reduced as depicted in Figure 8 by the blue and red distributions. But even so, when the number of dead actuators reaches 100, the total surface accuracy has reached 0.8 mm or more. In fact, it has been unable to meet the needs of high-frequency K-band (22 GHz) observation.

Table 2 Panel Type

Panel type	Number of panels	Number of nodes	Ratio of single panel area to equilateral triangle panel
A	42	55	~ 1.5
B	42	55	Inner - Outer ~ 1.5
C	60	73	Inner - Outer ~ 0.83
D	54	37	1

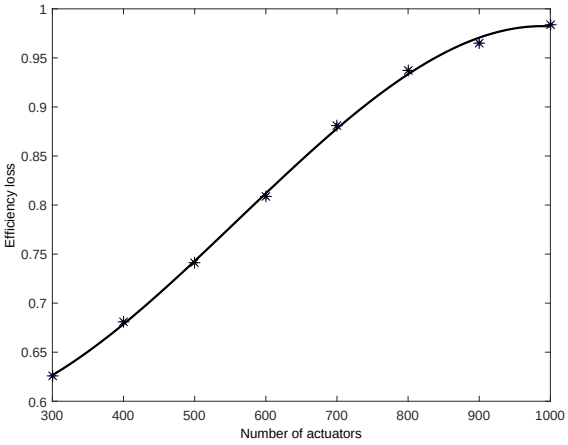

Fig. 5 The relationship between the efficiency loss and the number of actuators when El=17 deg.

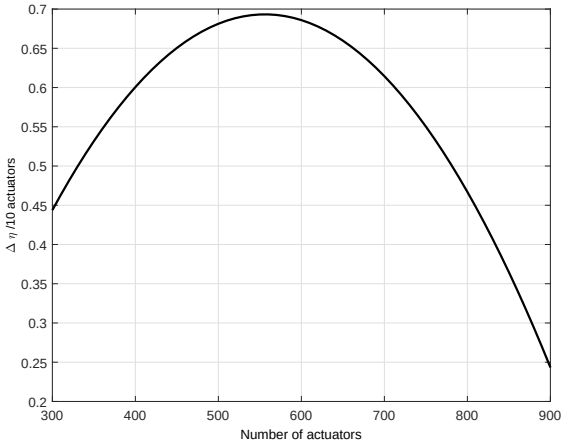

Fig. 6 The efficiency increase caused by every 10 actuators when El=17 deg.

4 PANEL TYPING ANALYSIS

4.1 Triangular Panel

The following is a quantitative analysis of different divisions of panels that compose rings. Figure 9 displays the projection of the panels on the aperture surface. It mainly compares the number of panels in the case of triangular panel division and equiangular division when the area of the aperture and the number of panel rings are almost the same. The number of nodes is just the number of actuators in the active surface condition. In

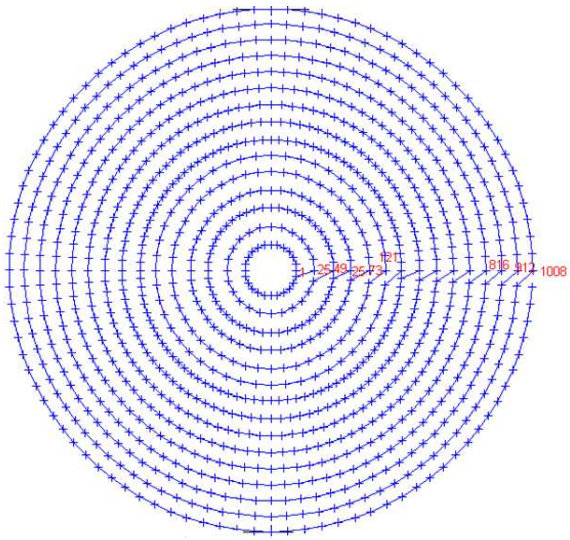

Fig. 7 The distribution of actuators on the Tianma 65 meter radio telescope.

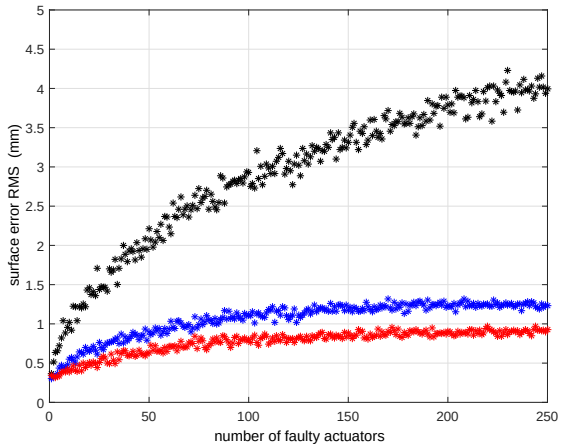

Fig. 8 The number of faulty actuators versus the aperture error.

order to achieve the optimal surface accuracy, control and cost, the area of a single panel should be as small as possible, and the number of actuators should be as small as possible. Figure 10 shows a 60 degree sector, three traditional equiangular segmentation methods and triangular segmentation methods. It can be seen from Table 2 that the panel segmentation method of C has a maximum number of 60 panels and a single panel has the smallest area. The theoretical surface shape control

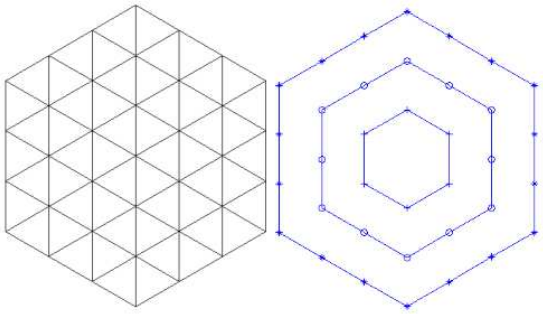

Fig. 9 *Left*: Equilateral triangle panels are assembled into three circles; *Right*: Circle dividing line for the panels.

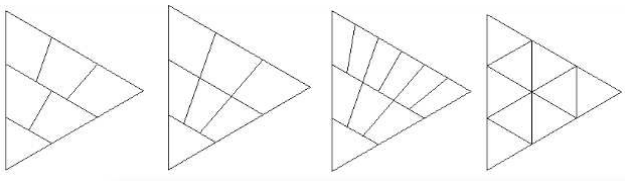

Fig. 10 Six equiangular divisions A, B and C and regular triangular division D.

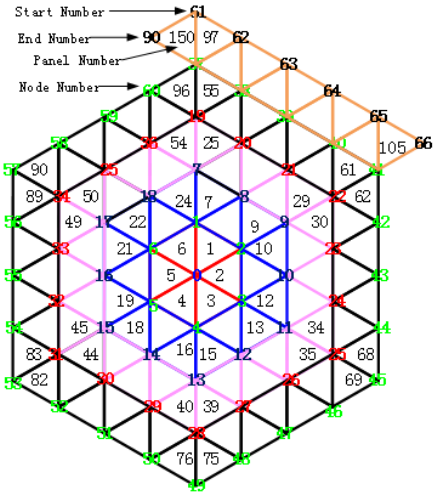

Fig. 11 Indexes of triangular panels.

accuracy will be the highest, but the number of nodes is also the highest which reaches 73. The triangle division method has 54 panels, which is 6 less than C, and the

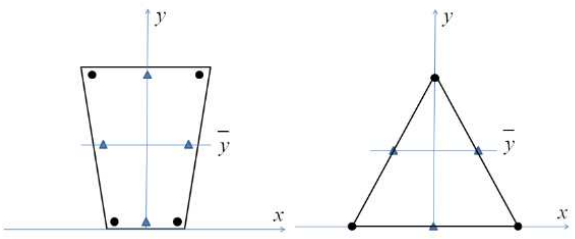

Fig. 12 *Left*: Trapezoidal panel adjustment points; *Right*: Triangular panel adjustment points.

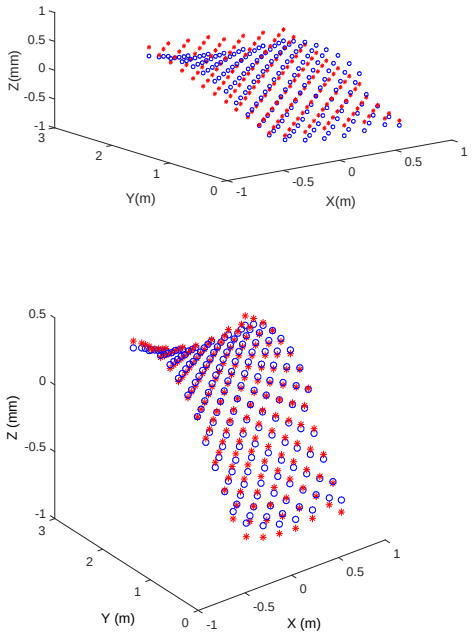

Fig. 13 Single panel fitting comparison.

number of nodes is only 37, less than half that of C. It can be seen that the advantage of triangular panel splicing is that it can effectively reduce the area of a single panel while sharply reducing the number of control nodes. This advantage becomes more obvious when the number of panel rings increases. In the traditional equiangular division method, the difference in area between an inner and outer single panel is generally large. This will not only cause uneven deformation of the inner and outer panels, but also will cause the outer edge of the backup frame to be too large and the stiffness of the outer rings to deteriorate, ultimately affecting the panel adjustment accuracy. The analysis method of the triangular panel appeared in the initial design of the Large Millimeter Telescope (LMT) (Baars & Kärcher 2018), while the practical application was carried out in the Square Kilometre Array (SKA) intermediate frequency antennas (Dewdney et al. 2009).

4.2 Index of Triangular Panel

It can be seen from Table 2 above that the triangular panel type has a relatively large advantage for reducing the number of actuators. But after adopting this type of panel, the indexing method of the panel and the node is more complicated than that of the trapezoidal panel. Here we need to discuss the indexing method of the nodes and the panels. Figure 11 is an example. The index law of panel number and node number is studied mainly based on the number of panels on each ring. Table 3 summarizes the index formula and calculation examples.

Table 3 Index of Triangular Panels

Rings	Panels	Nodes	Start node	End node
n	6(2n-1)	6n	$6\sum_{i=1}^{n-1} i+1$	$6\sum_{i=1}^{n} i$
1	6	6	1	6
2	18	12	7	18
3	30	18	19	36
4	42	24	37	60
5	54	30	61	90
23	270	138	1519	1656

4.3 The Surface Shape Calculation for a Single Panel

For the panel installed on the antenna, we need to calculate the adjustment to maintain the overall approximation (shape) of a parabola. We also need to diagnose the internal deformation of a single panel. For the measurement and adjustment of the trapezoidal panel, the Y and X axis rotations (i.e. slope) α and β respectively, in addition to l of the translation item, are traditionally used (Rochblatt 1991). The core aspect of this method is to regard the panel as a rigid plane to achieve a solution, which is commonly implemented in engineering applications. Since the trapezoidal panel is supported by at least four points, internal deformation is inevitable, so the torsion term inside the panel can actually be added. The fitting model is different from a traditional rigid panel (von Hoerner 1981). It can reduce the fitting error and is more in line with the actual situation of statically indeterminate installation of the panel. The following coordinate system can be employed. When the Z-direction displacement of each point inside the panel is measured, the model can be used to perform the least squares fitting of a single panel. The best adjustment of the four corners can be solved from the fitting. When the panel area is large, more adjustment points can be added, as shown in the left panel of Figure 12. In this case, the model can increase the number of parameters X^2 and Y^2 to make the fitting accuracy higher. We can establish a complete single panel adjustment amount fitting model as demonstrated in Equation (2) (Lei 2000).

$$z(x,y) = l+\alpha x+\beta(y-\overline{y})+\tau xy+\gamma x^2+\lambda(y-\overline{y})^2 \quad (2)$$

Among them: $\overline{y}$ is the midpoint position of the Y-direction panel. This amount is subtracted to solve the coupling. If it is not subtracted, it will cause additional contributions to the panel in the Z-direction. By comparing the solution results of many trapezoidal panels on the Tianma 65 meter radio telescope, the fitting error of a single panel is significantly reduced after the torsion term and the square term are included. Figure 13 displays the fitting comparison diagram of a panel. The left figure is the traditional rigid panel fitting method, and its fitting error (root mean square, RMS) is 0.12 mm. The right figure is the fitting method using Equation (2). The total error is 0.03 mm.

Compared with a trapezoidal panel, in addition to the advantages mentioned above, a main disadvantage of the triangular panel is also obvious. Because a triangular panel has fewer adjustment points, it can only do three point adjustment (X and Y slope term plus translation term). It is not suitable for four parameter fitting surface (including XY cross fitting term) to obtain better adjustment. However, as long as the processing accuracy of the triangular single panel is guaranteed and the area is not large, the XY cross term is actually not large. When the area of the triangular panel increases, it can be appropriate to increase the adjustment point, as depicted in the right panel of Figure 12, which can achieve a method similar to Equation (2) that improves the accuracy of the adjustment. In addition to giving the amount of adjustment for the panel, this method can also be used to accurately diagnose the deformation inside a single panel.

5 SUMMARY AND DISCUSSION

This article mainly studies the distribution method of actuators and the method of panel division. We tried to achieve the best surface accuracy control with the fewest actuators. By adopting the surface gravity FEM model and illumination design, the distribution of the actuators can be optimized. A triangular panel can then effectively reduce the number of actuators. The influence of the number of faulty actuators on the surface shape accuracy is demonstrated. A uniformly illuminated antenna has the highest requirements for reliability of the actuators. This paper presents the triangular panel and node index method as well as the fitting solution method for a single panel. This method provides a reference for the design of active surfaces or deformable sub-reflectors for large radio telescopes.

References

Baars, J. W. M., & Kärcher, H. J. 2018, Radio Telescope Reflectors, 447 (Springer International Publishing AG)
Dewdney, P. E., Hall, P. J., Schilizzi, R. T., & Lazio, T. J. L. W. 2009, IEEE Proceedings, 97, 1482
Dong, J., Zhong, W., Wang, J., et al. 2018, IEEE Transactions on Antennas and Propagation, 66, 2044
Lei, X. Y. 2000, in Finite Element Method (in Chinese), 131
Rochblatt, D. J. 1991, Telecommunications and Data Acquisition Progress Report, 108, 235
Ruze, J. 1966, IEEE Proceedings, 54, 633
von Hoerner, S. 1981, IEEE Transactions on Antennas and Propagation, 29, 953
Wang, J., Zhang, J., Fan, Q., et al. 2019, Scientia Sinica Physica, Mechanica & Astronomica, 49, 109501
Wang, J.-Q., Zhao, R.-B., Jiang, Y.-C., et al. 2020, RAA (Research in Astronomy and Astrophysics), 20, 009